Investigational New Drugs (2019) 37:602–615
https://doi.org/10.1007/s10637-018-0657-y

PRECLINICAL STUDIES

Hexane partition from *Annona crassiflora* Mart. promotes cytotoxity and apoptosis on human cervical cancer cell lines

Viviane A. O. Silva[1] · Ana Laura V. Alves[1] · Marcela N. Rosa[1] · Larissa R. V. Silva[1] · Matias E. Melendez[1] · Fernanda P. Cury[1] · Izabela N. F. Gomes[1] · Aline Tansini[1] · Giovanna B. Longato[2] · Olga Martinho[1,3,4] · Bruno G. Oliveira[5] · Fernanda E. Pinto[5] · Wanderson Romão[5] · Rosy I. M. A. Ribeiro[6] · Rui M. Reis[1,3,4]

Received: 5 June 2018 / Accepted: 14 August 2018 / Published online: 29 August 2018

Summary

Cervical cancer is the third most commonly diagnosed tumor type and the fourth cause of cancer-related death in females. Therapeutic options for cervical cancer patients remain very limited. *Annona crassiflora Mart.* is used in traditional medicine as antimicrobial and antineoplastic agent. However, little is known about its antitumoral properties. In this study the antineoplastic effect of crude extract and derived partitions from *A. crassiflora* Mart in cervical cancer cell lines was evaluated. The crude extract significantly alters cell viability of cervical cancer cell lines as well as proliferation and migration, and induces cell death in SiHa cells. Yet, the combination of the crude extract with cisplatin leads to antagonistic effect. Importantly, the hexane partition derived from the crude extract presented cytotoxic effect both *in vitro* and *in vivo*, and initiates cell responses, such as DNA damage (H2AX activity), apoptosis via intrinsic pathway (cleavage of caspase-9, caspase-3, poly (ADP-ribose) polymerase (PARP) and mitochondrial membrane depolarization) and decreased p21 expression by ubiquitin proteasome pathway. Concluding, this work shows that hexane partition triggers several biological responses such as DNA damage and apoptosis, by intrinsic pathways, and was also able to promote a direct decrease in tumor perimeter *in vivo* providing a basis for further investigation on its antineoplastic activity on cervical cancer.

Keywords *Annona crassiflora* Mart · Natural compounds · Hexane partition apoptosis · Cytotoxity and cervical cancer cell lines

Introduction

Cervical cancer is considered an important public health problem worldwide, representing the third most common cancer type among women [1, 2]. In addition to its high incidence, this tumor is usually diagnosed at advanced stages, which hampers effective treatment, especially in developing countries [2]. Cisplatin (cis-diamminedichloroplatinum) is the most used chemotherapeutic agent, generally applied concomitantly to radiotherapy. Despite constituting a potent antineoplastic, this

Ana Laura V. Alves and Marcela N. Rosa contributed equally to this work.

Electronic supplementary material The online version of this article (https://doi.org/10.1007/s10637-018-0657-y) contains supplementary material, which is available to authorized users.

✉ Rui M. Reis
rreis@med.uminho.pt

[1] Molecular Oncology Research Center, Barretos Cancer Hospital, Barretos 14784400, São Paulo, Brazil

[2] Research Laboratory in Cellular and Molecular Biology of Tumors and Bioactive Compounds, San Francisco University, Bragança Paulista 12916900, São Paulo, Brazil

[3] Life and Health Sciences Research Institute (ICVS), School of Medicine, University of Minho, Braga 4710057, Portugal

[4] ICVS/3B's - PT Government Associate Laboratory, Braga/Guimarães 4806909, Portugal

[5] Petroleomic and Forensic Laboratory, Chemistry Department, Federal University of Espírito Santo, Vitória 29075-910, ES, Brazil

[6] Laboratory of Experimental Pathology, Federal University of São João del Rei—CCO/UFSJ, Divinópolis 35501-296, Brazil

compound is associated to several side effects as well as patient resistance [3]. These facts have limited the clinical utilization of cisplatin, which has been directed towards combination therapies aiming to reduce the dose administered to the patient [3]. In this context, novel chemotherapeutic agents are of great interest to improve cancer therapy.

Medicinal plants represent an immense source for drug discovery. Many drugs currently employed as gold standard in tumor therapy have a natural origin or are direct derivatives of natural compounds [4]. They include epipodophyllotoxins, vinca alkaloids, camptothecin derivatives and taxanes [4, 5]. Nevertheless, it is estimated that less than 2% of the higher plants have their antineoplastic activity analyzed, owing to the time and intensive resources necessary for drug discovery process [6, 7]. The biodiversity found in Brazil is among the largest in the world (20–22% of the total), offering a broad range of opportunities for the production of plant medicines. Among the plant families found in the Brazilian Cerrado biome, *Annonaceae* comprises 29 geners [8, 9], of which *Annona* includes approximately 166 species of trees and shrubs [9, 10].

Among the species of the genus *Annona*, *A. crassiflora* Mart., 1841 (*Annonaceae*), commonly known as araticum, has several applications in the popular medicine [9]. Its leaves, bark, fruits and seeds have been widely used as invigorating, anti-inflammatory, antimalarial and antidiarrheal agents, in addition to chemopreventive action [11, 12]. Recently, the methanolic leaf extract as well as the seed extract of *A. crassiflora,* have demonstrated *in vitro* antiproliferative properties in several tumor types (glioblastoma, leukemia and lung, colorectal, ovarian cancer cell lines) [13]. Moreover, it has been reported that an acetogenin-rich fraction of the ethanolic extract from wood of *A. crassiflora* promotes toxicity and antitumor activity in Ehrlich tumors [14]. These works have raised the interest in *A. crassiflora* in the oncology field, but more studies are needed to elucidate its whole therapeutic antitumor potential.

In the present study we determined the biological effect of total leaf extract from *A. crassiflora* Mart. in a panel of cervical cancer cell lines. In addition, the hexane partition derived from the extract was also characterized *in vitro* about functional and molecular mechanisms as well as *in vivo* model of cervical cancer.

Material and methods

Crude extract preparation

The crude extract from *A. crassiflora* was obtained by the Federal University of São João del-Rei (SJDRFU) (Centro-Oeste Dona Lindu Campus-MG). The leaves of *A. crassiflora* were collected on Cerrado area (S 18° 58′ 08“ and W 49° 27’ 54”) and identified by Dr. Arali Aparecida Costa Araujo and deposited in the Herbarium of the Botany Department of Federal University of Minas Gerais (143400). The samples collected were washed, cut and dried for 5 days at room temperature. After that, the samples were submitted of extraction with ethylic alcohol 70% (1:5 by 5 days). The crude extract liquid obtained was filtrated, froze and submitted to freeze-drying. The crude extract was initially dissolved in dimethyl sulfoxide (DMSO) at concentration of 50 mg/mL and stored at −20 °C.

Partitioning preparation

After results obtained with the crude extract, the partitioning preparation was carried out by SJDRFU using 4 different solvents with increases polarity: A- Hydroalcoholic, B- Hexane, C- Chloroform and D- Ethyl acetate. The partitions were submitted at freeze-drying. Studies from our group revealed that the hexane partition has one of the highest cytotoxic bioactivities (data not shown). Then, the hexane partition was also dissolved in DMSO at a concentration of 25 mg/mL and stored at −20 °C. The intermediate dilutions of the hexane partition were prepared to obtain a concentration of 1% DMSO.

Analysis of secondary compounds present in the hexane partition in *Annona crassiflora* Mart by FT-ICR MS

The hexane partition was analyzed using the negative ion-mode Electrospray Ionization Fourier Transform Ion Cyclotron Resonance Mass Spectrometer (ESI (−) FT-ICR MS, model 9.4 T Solarix, Bruker Daltonics Bremen). All mass spectra were externally calibrated using NaTFA (*m/z* from 200 to 2000). The parameters of the ESI (−) source were: nebulizer gas pressure of 0.5–1.0 bar, capillary voltage 3–3.5 kV and capillary transfer temperature 250 °C. The mass spectrum used Compass Data Analysis *software*. The resolution power used was $m/\Delta m_{50\%} \cong 200{,}000$ (where $\Delta m_{50\%}$ is the maximum peak width at peak height $m/z \cong 400$) and mass accuracy <8 ppm. The degree of unsaturation for each molecule can be deduced directly from its DBE value according to the equation DBE = c - h/2 + n/2 + 1, where c, h, and n are the numbers of carbon atoms, hydrogens, and nitrogen in the molecular formula, respectively. The FT-ICR mass spectrum was acquired and processed using Compass Data Analysis *software.* The elemental compositions of the present compounds were determined by measuring the *m/z* ratio values. The proposed structures for each formula were determined using the ChemSpider database (www.chemspider.com) and the Dictionary of Natural Products database (http://dnp.chemnetbase.com).

Cell lines and cell culture

Seven immortalized human cervical cancer cell lines model obtained from *European Collection of Cell Cultures* (ECACC, Salisbury, United Kingdom) were analysed, being then: HtTA-1, HR5, HeLa, SiHa, BU25TK, HR5-CL11 and CaSki. The identity of all cell lines was confirmed by genotyping and further tested for micoplasma presence through *MycoAlert*^{Tm}*Mycoplasma Detection Kit* (Lonza), following the manufacturer's instructions [15]. All cell lines were maintained in Dulbecco's modified Eagle's medium (DMEM 1X, high glucose; Gibco, Invitrogen) supplemented with 10% fetal bovine serum (FBS) (Gibco, Invitrogen) and 1% penicillin/streptomycin solution (P/S) (Gibco, Invitrogen), at 37 °C and 5% CO_2, until confluence. Posteriorly, the cells were trypsinized (0.05% trypsin/0.53 mM EDTA - *TripLE Express*, Life Technologies), plated and maintained under the conditions described above for the biological characterization and therapeutic response studies.

Cell viability assay

The cytotoxicity effect of crude extract and hexane partition were *assessed by* Cell Titer 96 Aqueous cell proliferation assay (MTS assay, PROMEGA, Madison, WI, USA) as previous described and following the manufacturer's instructions [15, 16]. Briefly, cells were plated into 96-well plates, treated with increasing concentrations of the samples (crude extract: 1.5 μg/mL to 300 μg/mL, cisplatin: 0.12 μg/mL to 30 μg/mL and hexane partition: 2.5 to 200 μg/mL) diluted in DMEM (0.5% FBS) or vehicle (1% DMSO) and incubated for 72 h. Absorbance of samples was measured in automatic microplate reader Varioskan (Thermo) at 490 nm. The datas were expressed as mean viable cells relatively to DMSO alone (represented as 100% viability) ± SD. Half maximal inhibitory concentration (IC_{50}) values were determined using the non-linear regression curve using GraphPad PRISM version 7 (GraphPad Software, La Jolla California USA).

Clonogenic- assay

Inhibition of anchorage-independent growth of tumor cells was assessed by soft-type-agar assay as we previously reported [16, 17]. Briefly, 5×10^3 SiHa cells was treated every 2 days by DMEM medium (0.5% FBS) containing crude extract or hexane partition (at IC_{50} concentrations) during 20 days and colonies formed were stained with 0.05% crystal violet for 15 min. Photo-documented colonies were analyzed using the *Image J* software (National Institutes of Health; http://rsbweb.nih.gov/ij/). The assay was performed in two biological replicates and the experiments were done in duplicate.

Wound-healing migration assay

Cell migration properties were evaluated by wound-healing assay, as previously described by our group [16, 18]. SiHa cells were treated with crude extract at IC_{50} concentration and photographed by phase contrast microscopy (Model IX71 Olympus) to evaluate wound closure at 0, 24, 48 and 72 h after treatment. The percentage of relative migration distance was calculated as wound area at a given time compared to the initial wound surface. Pictures shown are representative of three independent experiments performed in triplicates.

Drug combination studies

Combination drug studies were done using all cell lines with a fixed concentration of cisplatin (**Sigma Aldrich), representing its** IC_{50} value, and increasing concentrations of crude extract [16]. Drug interactions were evaluated by the combination index (CI) that was calculated by the Chou–Talalay equation, which takes into account both the potency (Dm or IC_{50}) and the shape of the dose–effect curve [19], using CalcuSyn software version 2.0 (Biosoft; Ferguson, MO, USA). In CI analysis, synergy was defined as CI values significantly lower than 1.0; antagonism as CI values significantly higher than 1.0; and additivity as CI values equal to 1.0 at drug IC_{50} value for each cell line.

Western blot-analysis

Survival/proliferation, death and cell cycle signaling pathways were evaluated by western-blot as as previously described [16]. For this approach, after 24 h of treatment, protein extracts by SiHa cells treated with 15 μg/mL of both, crude extract and hexane partition, were separated by 10% SDS-PAGE and incubated with cleaved anti-PARP (1:1000), anti-caspase 3, 7, 8 and 9 (1: 1000), anti-ERK (1:1000), anti-pERK (1:1000), anti-AKT (1:1000), anti-AKT (1:1000), anti-pH2AX (1:500), anti-H2AX (1:500) and anti-p21 (1:1000), all purchased from Cell Signaling.

To validate the results obtained, SiHa cells were pre-treated for 1 h with MG132 10 μM and N-Acetyl-Cysteine (NAC) 2 mM prior to treatment with the partition. After 24 h of treatment, protein extracts were blotted against the primary antibodies described above and their corresponding peroxidase-conjugated secondary antibody. The membranes were then incubated with *ECL (*GE) and revelaed by chemiluminescence method. Chemiluminescent detection was performed on *Image Quant LAS*4000 mini photo documentation system (GE Healthcare Life Sciences). Labeled bands were subsequently analyzed and quantified using the *Image J* software (National Institutes of Health; http://rsbweb.nih.gov/ij/).

Determination of mitochondrial depolarization

SiHa cells were plated in 6-well plates until reach 100% confluence. Cells were then incubated with the hexane partition at the concentration of 15 μg/mL. After 24 h, cells were subjected to *MitoStatus RED* (BD Biosciences) labeling, as recommended by the manufacturer. Data acquisition was performed on *BD FACSCanto II* (BD Biosciences) and analyzed with BD FACSDiva software (BD Biosciences). Data shown are representative of two independent experiments performed in duplicates.

In vivo characterization of the hexane partition effect on tumor growth and angiogenesis

The hexane partition effect on the proliferative and angiogenic potential of cervical cancer cells was evaluated by the corialantoid membrane (CAM) assay as previously described [18]. The eggs used were subdivided into four groups: *group I*, inoculated only DMSO (partition vehicle); *group II*, inoculated with the hexane partition; *group III*, inoculated with SiHa tumor cells and treated with DMSO; and *group IV*, inoculated with the SiHa cells and treated with the hexane partition. At the tenth day of development, a small plastic ring was inoculated onto CAM in groups I and II whereas tumor cells (SiHa – 2×10^6 cells) were inoculated into 20 μL of DMEM medium without FBS and 20 μl matrigel (Corning) in groups III and IV. The eggs were kept in the incubator and on the fourteenth day of development, groupsx I, II, III and IV were photodocumented *in ovo* using an *Olympus SZX16* stereomicroscope and *Olympus DP71* digital camera. Then, groups I and III received 20 μL DMEM medium containing 0.5% FBS with DMSO (control eggs) while groups II and IV received 20 μl of DMEM (0.5% FBS) medium and 15 μg/mL of the hexane partition. On the seventeenth day (72 h of incubation with the samples), the rings and tumors were again photodocumented, *in ovo*. The fertilized eggs were then euthanized at −80 °C for 10 min. Moreover, tumors or CAM containing the ring were fixed with 3.7% paraformaldehyde and photodocumentated *ex ovo*. To confirm the death of the embryos, parameters described by "AVMA Guidelines for the Euthanasia of animals: 2013 (Leary, Underwood et al. 2013)" were followed.

Tumor perimeter was measured on the fourteenth and seventeenth day using *ImageJ* software (National Institutes of Health; http://rsbweb.nih.gov/ij/) and the results were expressed as mean percentage of tumor growth in each group, relative to the fourteenth day ± standard deviation (SD). For blood vessel counts, images performed on the seventeenth day were counted *ex ovo* and results expressed as mean vessel count in each treated group. Both results were expressed as mean of three independent experiments. This study was approved by the Committee on Ethics in the Use of Animals (CEUA) of the Institution (number: 028/2016).

Statistical analysis

Results of *in vitro* and *in vivo* experiments are expressed as mean ± SD of three independent experiments. Student's t test was applied for comparing two conditions, whereas two-way analysis of variance (ANOVA) was used for assessing differences between more groups. *p*-values <0.05 were considered significant. All statistical analyses were performed using GraphPad PRISM version 7 (GraphPad Software, La Jolla California USA).

Results

Biological characterization of the crude extract from *A. crassiflora*

Crude extract from *A. crassiflora* promotes cytotoxicity in cervical tumor cells

To evaluate the cytotoxicity of crude extract *in vitro*, the IC_{50} was determined in a panel of immortalized cervical cancer cell lines. The screening revealed that the crude extract had a lower cytotoxic activity in all the cells evaluated when compared to cisplatin (Table 1). Based on the cytotoxicity profile, the lines HtTa-1 and SiHa were considered sensitive and resistant, respectively. The IC_{50} values for HtTa-1 were 3.40 μg/mL for the crude extract and 21.10 μg/mL for cisplatin. For SiHa, the obtained values were 39.88 μg/mL for the crude extract and 14.95 μg/mL for cisplatin (Table 1). The other cervical lines (HR5, HR5Cl-11, HeLa, CaSki and Bu25TK) also exhibited decrease in cell viability and dose-dependent effect upon treatment with the compounds (data not shown).

The efficacy of the crude extract in combination with cisplatin was also tested. The present results showed that, when combined, the crude extract and cisplatin seems to have an antagonistic effect (combination index (CI > 1) for the majority of the investigated cervical tumor cell lines (Table 1).

Crude extract of *A. crassiflora* shows antiproliferative potential and inhibits cell migration

To determine whether the reduction in cell viability derived from decrease in proliferation rate, the clonogenic

Table 1 Comparison of the mean IC_{50} values of crude extract, cisplatin and hexane partition in cervical cancer cell lines

Cell line	Crude extract Mean $IC_{50} \pm$ S.D. (μg/mL)	Cisplatin Mean $IC_{50} \pm$ S.D. (μg/mL)	Combination index (CI)[a]	Hexane partition Mean $IC_{50} \pm$ S.D. (μg/mL)
HtTA-1	3.40 ± 3.60	21.10 ± 0.99	27.9	0.47 ± 0.05
HR5	15.31 ± 0.07	0.01 ± 1.63	3.02	0.49 ± 0.19
HR5CL-11	16.71 ± 0.03	1.96 ± 1.92	1.4	0.18 ± 0.07
HeLa	17.46 ± 0.43	6.39 ± 1.80	2.17	5.67 ± 1.49
CaSki	7.48 ± 0.42	1.91 ± 1.08	19.12	ND
Bu25TK	13.94 ± 0.99	11.60 ± 0.04	2.22	11.65 ± 1.20
SiHa	39.88 ± 0.74	14.95 ± 3.62	4.24	14.71 ± 1.55

ND Not determined

[a] Drug combination studies were done with cisplatin and crude extract. The CI was analyzed using CalcuSyn Software version 2.0. The CI value significantly lower than 1.0, indicates drug synergism; CI value significantly higher than 1.0, drug antagonism; and CI value equal to 1.0, additive effect

potential of treated cells was evaluated. The assay demonstrated a drastic reduction ((56% for HtTA-1 (sensitive) and 70% for SiHa (resistant)) in the number of colonies formed after treatment with the crude extract compared to control group (Fig. 1a, b). In addition, using the wound-healing assay we evaluate the effect of the crude extract on SiHa migration, and observed that it promoted attenuation of migration over time, with a significant decrease of 80% ($p < 0.05$) in comparison to the control cells at 72 h (Fig. 1c, d).

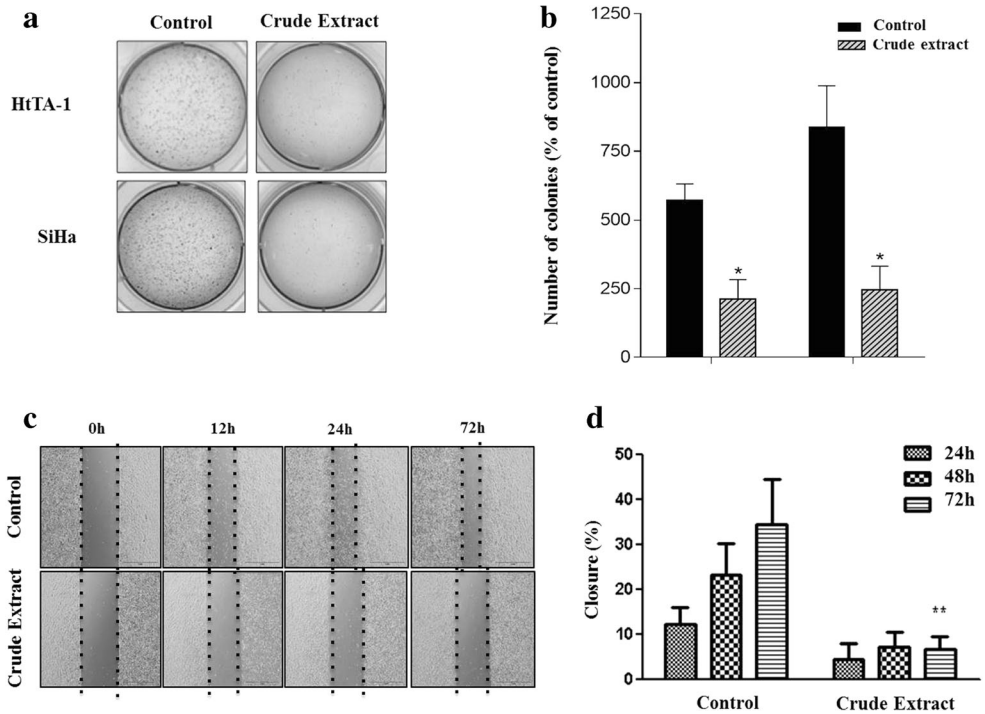

Fig. 1 Effect of crude extract on anchorage independent growth and migration in cervical cancer cell lines. **a** Representative images of colony assay of SiHa and HtTA-1 cell lines exposed to crude extract (40 μg/mL and 3.4 μg/mL, respectively). The cells were tested for their ability to proliferate in growth medium containing 0.35% agar. The formation of multicellular colonies was photographed after 20 days of treatment with the crude extract. The figure is representative of two independent experiments performed in duplicate. **b** Graph of the data are represented as mean ± SD and differences with p <0.05 in the Student's t test (*). **c** Representative images of wound healing assay of SiHa cell line after 24 hours, exposed to the crude extract (40 μg/mL). A standardized (wound) zero was applied to the monolayer and scanned images were taken at various time points (0, 24, 48 and 72 hours). The experiments were performed three times independently and in duplicate. **d** Bars represent the relative migration expressed as the mean ± SD and differences with p <0.005 in the Student's t-test (**)

Table 2 Proposed structures by ESI(−)FT-ICR MS for hexane partition in *A. crassiflora* Mart

m/z mesured	m/z *theoretical*	Error (ppm)	DBE	$[M-H]^-$	Proposed compound	Reference
255.2332	255.23324	−1.12	1	$[C_{16}H_{32}O_2$- H]$^-$	palmitic acid	[20]
277.21897	277.21894	6.01	4	$[C_{18}H_{30}O_2$-H]$^-$	octadecatrienoic acid	[21]
279.23448	279.2344	6.58	3	$[C_{18}H_{32}O_2$-H]$^-$	coriacyclodienin	[22]
281.24992	281.24899	4.7	2	$[C_{18}H_{34}O_2$-H]$^-$	nornuciferina	[23]
283.26637	283.26632	8.79	1	$[C_{18}H_{36}O_2$-H]$^-$	annoglaucin	[24]
293.21101	293.21098	2.12	4	$[C_{18}H_{30}O_3$-H]$^-$	rolliniastatin	[25]
309.20739	309.20733	9.9	2	$[C_{18}H_{34}O_3$-H]$^-$	hydroxydehydronuciferine	[26]
315.25144	315.25132	9	1	$[C_{18}H_{36}O_4$-H]$^-$	caffeine of α-terpineol	[27]
325.19395	325.19365	1.83	4	$[C_{19}H_{30}O2$-H]$^-$	norglaucine	[28]
329.23289	329.23271	1.04	2	$[C_{19}H_{34}O5$-H]$^-$	rollitacin	[22, 29]
395.38339	395.3832	11.9	1	$[C_{26}H_{52}O_2$-H]$^-$	β-sitosterol	[30]
423.32499	423.32445	0.89	8	$[C_{29}H_{44}O_2$-H]$^-$	polycarpol	[30]
445.35916	445.35859	1.04	8	$[C_{27}H_{42}O_5$-H]$^-$	cyclosenegalin A	[32]
471.34435	471.34425	6.92	7	$[C_{27}H_{42}O_5$-H]$^-$	reticulacinone	[33]
505.22051	505.22045	2.34	23	$[C_{37}H_{30}O_2$-H]$^-$	tryptamine	[34]
591.26044	591.26042	1.04	22	$[C_{37}H_{69}O_5$-H]$^-$	Catechin metylated	[35]
619.28834	619.26784	1.24	20	$[C_{37}H_{64}O_7$-H]$^-$	goniotriocin	[22]
651.28013	651.24741	0.5	15	$[C_{36}H_{44}O_{11}$-H]$^-$	Coriaheptocin	[36]
709.49049	704.45012	1.69	6	$[C_{40}H_{70}O_{10}$-H]$^-$	procyanidin	[37]
834.74642	834.65471	1.24	6	$[C_{42}H_{70}O_{10}$-H]$^-$	rhamnopyranosyl	[38]

Characterization of the hexane partition from *A. crassiflora*

The hexane partition from *A. crassiflora* contains acids palmitate, octadecatrienoic acetogenins and alkaloids in their constituition

Studies from our group revealed that the hexane partition has one of the highest cytotoxic bioactivities (data not shown). Thus, we evaluated the profile of secondary compounds identified in the hexane partition of *A. crassiflora* via FT-ICR MS analysis (Table 2). Twenty secondary compounds were identified in their deprotonated form, $[M-H^+]^-$ ions corresponding to compounds: palmitic acid, $[C_{16}H_{32}O_2$-H]$^-$ of *m/z* 255 (compound 1); octadecatrienoic acid, $[C_{18}H_{30}O_2$-H]$^-$ ion of *m/z* 277 (compound 2); coriacyclodienin, $[C_{18}H_{32}O_2$-H]$^-$ ion of *m/z* 279 (compound 3); nornuciferina, $[C_{18}H_{34}O_2$-H]$^-$ ion of *m/z* 281 (compound 4); annoglaucin, $[C_{18}H_{36}O_2$-$H^+]^-$ ion of *m/z* 283 (compound 5); rolliniastatin, $[C_{18}H_{30}O_3$-H]$^-$ ion of *m/z* 293 (compound 6); hydroxydehydronuciferine, $[C_{18}H_{34}O_3$-H]$^-$ ion of *m/z* 309 (compound 7); caffeine of α-terpineol, $[C_{18}H_{36}O_4$-H]$^-$ ion of *m/z* 315 (compound 8); norglaucine, $[C_{19}H_{30}O_2$-$H^+]^-$ ion of *m/z* 325 (compound 9); rollitacin, $[C_{19}H_{34}O_5$-H]$^-$ ion of *m/z* 329 (compound 10); β-sitosterol, $[C_{26}H_{52}O_2$-H]$^-$ ion of *m/z* 395 (compound 11); polycarpol, $[C_{29}H_{44}O_2$-H]$^-$ ion of *m/z* 423 (compound 12); cyclosenegalin A, $[C_{27}H_{42}O_5$-H]$^-$ ion of *m/z* 445 (compound 13); reticulacinone, $[C_{27}H_{42}O_5$-H]$^-$ ion of *m/z* 471 (compound 14); tryptamine, $[C_{37}H_{30}O_2$-H]$^-$ ion of *m/z* 505 (compound 15); catechin metylated, $[C_{37}H_{69}O_5$-H]$^-$ ion of *m/z* 591 (compound 16); goniotriocin, $[C_{37}H_{64}O_7$-H]$^-$ ion of *m/z* 619 (compound 17); Coriaheptocin, $[C_{36}H_{44}O_{11}$-H]$^-$ ion of *m/z* 651 (compound 18); procyanidin, $[C_{40}H_{70}O_{10}$-H]$^-$ ion of *m/z* 704 (compound 19); rhamnopyranosyl, $[C_{42}H_{70}O_{10}$-H]$^-$ ion of *m/z* 834 (compound 20). The *m/z* values of the main identified molecules are presented on Table 2 [20–38].

The hexane partition of *A. crassiflora* promotes cytotoxicity and reduces the proliferative potential of cervical cancer cell lines

The cytotoxicity assays showed that treatment with concentrations from 2.5 to 25 μg/mL of hexane partition reduced the cell viability of the cancer cell lines in a dose-dependent manner (Fig. 2a). Treatment with the hexane partition showed stronger effect on cell viability compared to the crude extract, in which reduced the IC_{50} average of values, from 16.32 μg/mL to 5.53 μg/mL (Table 1). This partition was also evaluated for its effect on anchorage-independent growth, and resulted in a reduction of more than 90% in the number of colonies formed after the treatment in comparison to control cells (Fig. 2b, c).

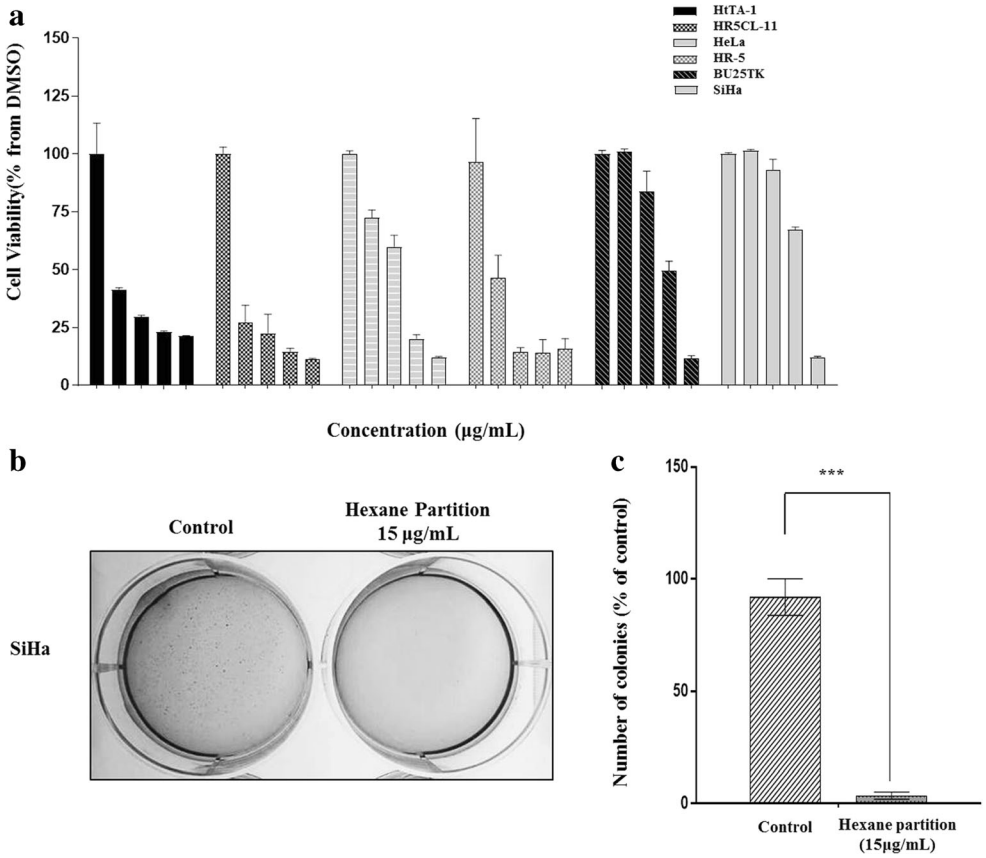

Fig. 2 Effect of hexane partition treatment on the cytotoxicity and anchorage independent growth in cervical cancer cell lines. **a** Cellular viability was measured at 72 hours by MTS assay. The results were expressed as the mean percentage ± SD of three independent experiments of viable cells relatively to the DMSO alone (considered as 100% viability). Data represent the mean of at least three independent experiments done in triplicate. **b** Representative images of colony assay of SiHa cell lines exposed to hexane partition (15 µg/mL). The SiHa cell line was tested for its ability to proliferate in growth medium containing 0.35% agar. The formation of multicellular colonies was photographed after 20 days of treatment with the hexane partition. The figure is representative of two independent experiment performed in duplicate. **c** Graph representing the number of colonies obtained in the control and treatment. The asterisks (***) indicate statistical significance ($p < 0.0001$) between control and experimental group in the Student's t test

Hexane partition modulates intracellular signaling pathways

To better characterize the effects of the hexane partition in important tumorigenesis signaling pathways (apoptosis, proliferation, survival and motility), the proteins PARP, ERK, AKT, H2AX and p21 were quantified after 24 h in SiHa cell line treated with crude extract and the hexane partition at 15 µg/mL (IC_{50} value for hexane partition).

We observed that only hexane partition promoted an increase in ERK activity, when compared to the DMSO control or the total extract groups. Moreover, no alteration was observed in AKT activity after both treatments when compared with DMSO control group, indicating that this protein possibly does not seen to belong to the signaling pathway modulated by the partition (Fig. 3a). However, when we treated the cells with the respective IC_{50} concentrations for the extract and cisplatin (40 and 15 µg/mL, respectively), we were able to see and increase in the activity of ERK and a reduction in the activity of the protein AKT only in the crude treated cells, which was validated in two different cell lines (Supplementary Fig. 1).

Hexane partition promotes p21 degradation via ubiquitin proteasome system

To further explore the extract and the partition effect in the intracellular signalling, we evaluated p21 protein expression, known important regulator of cell cycle as well as cell death regulation in response to DNA damage [39]. A decrease in p21 expression in the SiHa cell line was observed in both treatments compared (IC_{50} value for hexane partition - 15 µg/mL) to the control, suggesting an involvement in cell cycle modulation (Fig. 3b). Moreover, degradation of p21 was also observed with both crude and cisplatin at their IC_{50} concentrations in two different cell lines (Supplementary Fig. 1).

Decrease in p21 expression is reported to lead to cell cycle arrest, mediated by the ubiquitin proteasome system (UPS) [40]. Therefore, to verify this hypothesis, SiHa cells were

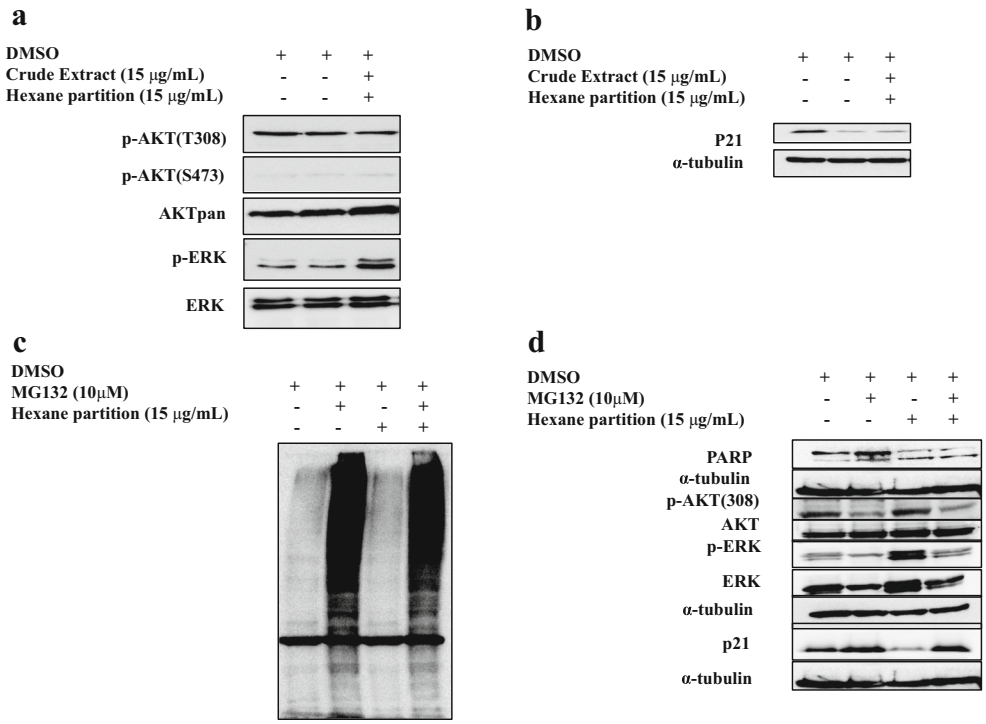

Fig. 3 Biological effect of crude extract and hexane partition treatment on cervical cancer cell proliferation, survival and cell cycle. **a** Representative images of western blotting from SiHa cells incubated with crude extract (15 μg/mL) and hexane partition (15 μg/mL) for 24 hours. Controls were treated with DMSO (1%). Total cell extracts from the same preparation were submitted to western-blotting analysis to evaluate the expressions of p-ERK, ERK, p-AKT and AKT proteins. **b** Representative images of western blotting from SiHa cells incubated with crude extract (15 μg/mL) and hexane partition (15 μg/mL) for 24 hours. Controls were treated with DMSO (1%). Total cell extracts from the same preparation were subjected to western-blotting analysis to evaluate p21 expression. **c** Effect of MG132 inhibitor pre-treatment on cervical cancer lines exposed to hexane partition. SiHa cells were pretreated with 10 μM of MG132 inhibitor for 1 hour and thereafter 15 μg/mL of the hexane partition. Controls were treated with DMSO (1%). Total cell extracts from the same preparation were subjected to western-blotting analysis to evaluate ubiquitin proteins expression. **d** Total cell extracts from the treatment of MG132 inhibitor pre-treatment on cervical cancer lines were submitted to western-blotting analysis to evaluate the PARP, p-AKT, AKT, p-ERK, ERK and p21, p-H2AX and H2AX. The α-tubulin protein are shown as an internal control

treated for 1 h with the proteasome inhibitor MG132 (10 μM), prior to treatment with the hexane partition. Ubiquitin antibody was used as control of the MG132 treatment (Fig. 3c). Our results revealed that inhibition of the UPS by MG132 (Fig. 3d) hindered the degradation of p21, indicating that treatment with the partition activates the ubiquitination system, responsible for modulation of p21 expression. Moreover, this effect correlated with the downregulation of ERK activity. No effect of MG132 was observed in AKT, nor in the PARP cleavage induced by the hexane partition treatment (Fig. 3d).

Hexane partition promotes apoptosis via intrinsic pathway

Our results demonstrated that treatment with the hexane partition and the crude extract triggered cleavage of caspases 3 and 9. Cleavage of PARP was also observed, suggesting induction of cell death (Fig. 4a). Moreover, it was also observed an increase PARP cleavage with both crude and cisplatin at IC_{50} concentrations in two different cell lines (Supplementary Fig. 1).

To further explore the apoptotic pathways involved, cleavage of caspase 8 and mitochondrial depolarization (ΔΨm) were evaluated. No alteration was observed in cleaved-caspase 8 in SiHa cells treated either with crude extract or hexane partition, when compared with DMSO control group (Fig. 4b).

Evaluation of mitochondrial membrane depolarization (ΔΨm), assayed with *MitoStatus Red* (BD Biosciences), revealed that treatment with hexane partition caused a decrease of 64.8% in positive cells of polarized mitochondrial membrane (from 87.7 to 22.9%) in comparison to the control. The largest part (77.1%) presented fluorescence intensity at the wavelength of 527 nm, indicating depolarization of the mitochondrial membrane of the cells (Fig. 4c, d). Hence, these results indicate that treatment with hexane partition, and with the extract (data not shown), triggers depolarization of the mitochondrial membrane, activating cell death via the intrinsic apoptotic pathway.

Hexane partition increases H2AX activity, triggered by ROS

It has been described that cell death can be initiated by cell damage and stress [41]. Therefore, the activity of H2AX protein was evaluated. Following 24 h of treatment, it was observed in both crude and hexane partition an expressive

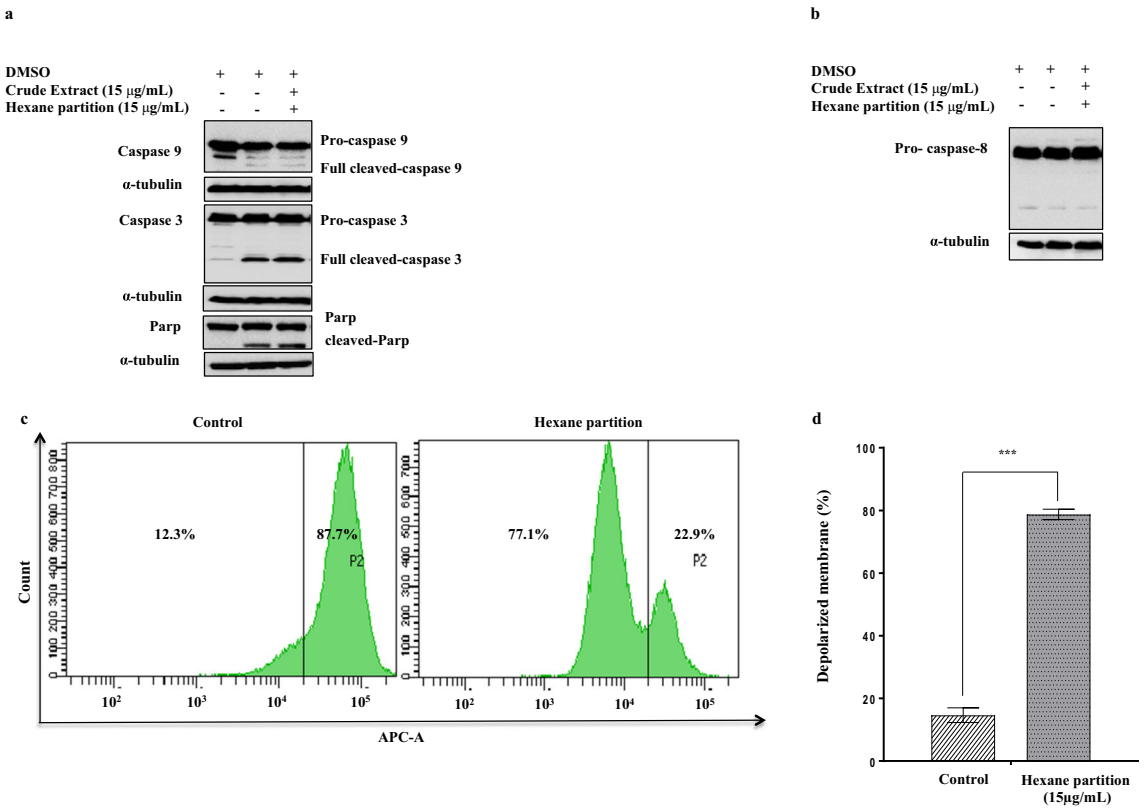

Fig. 4 Biological effect of crude extract and the hexane partition treatment on cervical cancer cell line cell death. **a** Representative images of western blotting from SiHa cells incubated with crude extract (15 μg/mL) and hexane partition (15 μg/mL) for 24 hours. Controls were treated with DMSO (1%). Total cell extracts from the same preparation were submitted to western-blotting analysis to evaluate the expression of caspase 3, 9 and PARP. **b** Total cell extracts from the same preparation were submitted to western-blotting analysis to evaluate the expression of caspase 8. α-Tubulin protein is shown as an internal control. n.s means that there was no significance. **c** Representative images of membrane mitochondrial depolarization was evaluated by flow cytometry after labeling SiHa cells with MitoStatus Red – untreated control and hexane partition treated cells after 24 hours. **d** Graph with the percentage of depolarized membrane. Data are representative of two experiments. Error bars represent SD. Graph of the data are represented as mean ± SD and differences with $p < 0.0001$ in the Student's t test were considered statistically significant (***)

increase in H2AX activity (Fig. 5a). Curiously, it was also observed an increase in H2AX expression with both crude and cisplatin at IC_{50} concentrations in two different cell lines (Supplementary Fig. 1), which may indicate DNA damage triggered by increase in reactive oxygen species (ROS) [42]. In this context, SiHa cells were pre-treated with 2 mM of *N-acetylcysteine* (NAC), a known antioxidant, prior to treatment with the hexane partition. Our results demonstrated that stress inhibition by NAC hindered H2AX activation, but was not able to modulate p21, PARP, ERK and AKT (Fig. 5b).

Hexane partition induces antitumor activity *in vivo*

To evaluate the effect of hexane partition treatment on proliferation *in vivo*, SiHa cells were inoculated into the chicken embryo CAM. From day 14 to day 17 of embryo development, we showed a mean growth of 165.3 ± 78.28 μm of tumors formed on the control group (III) (Fig. 6a, b). In contrast, tumors treated with hexane partition showed a reduction of 59.8 ± 32.1% of the tumor growth and on the treated group (IV) were − 137.2 ± 34.19 μm, respectively (DMSO, $n = 16$; hexane partition, $n = 17$) (Fig. 6a, b).

The number of blood vessels recruited to the tumors treated with hexane partition did not decreased compared to the tumors treated with control group (mean 97.56 ± 8.21 μm and 88 ± 5.97 μm blood vessels, respectively) (Fig. 6c). This result was confirmed when we compared the number of vessels in the absence of tumors; groups I and II (mean 119.5 ± 11.2 μm and 97 ± 7.84 μm, respectively) (Supplementary Fig. 2), indicating that in this CAM model, the hexane partition effect is anti-neoplastic rather than anti-angiogenic.

Discussion

Natural products constitute potential therapy alternatives for the treatment of various neoplasms, including cervical cancer [5, 6, 9]. In the present study, the cytotoxic and antineoplastic potential of the crude extract and hexane partition obtained

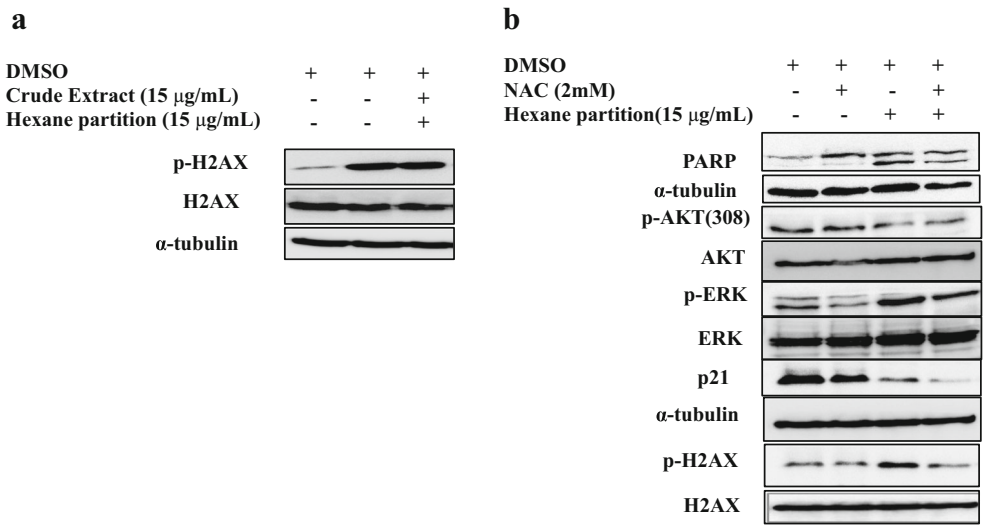

Fig. 5 Biological effect of crude extract and the hexane partition treatment on cervical cancer cell line cellular damage. **a** Representative images of western blotting from SiHa cells incubated with crude extract (15 μg/mL) and hexane partition (15 μg/mL) for 24 hours. Controls were treated with DMSO (1%). Total cell extracts from the same preparation were submitted to western-blotting analysis to evaluate the expression and activity of H2AX. **b** Effect of N-acetyl-L-cysteine (NAC) pre-treatment under the hexane partition biological effect in cervical cancer cell line. SiHa cells line were pretreated with 2 mM of the NAC antioxidant for 1 hour and then 15 μg/mL of the hexane partition. Total cellular extracts from the treatment were submitted to WB analysis to evaluate the expressions of PARP, p-AKT, AKT, p-ERK, ERK, p21, p-H2AX and H2AX expression. The α-tubulin protein is shown as an internal control

from leaves of the plant *A. crassiflora* Mart. derived from Brazilian cerrado bioma was investigated. Our results demonstrated dose-dependent cytotoxic effects of the crude extract in cervical cancer lines. According to the American NCI criteria, the crude extract of *A. crassiflora* has promising potential for new analyses, as long as the IC_{50} values are lower than 20 μg/mL for 48 h or lower than 30 μg/mL for 72 h (http://www.cancer.gov) [43, 44]. The cytotoxic effects promoted by the crude extract reflected in IC_{50} values lower than 30 μg/mL for five of the six tested tumor lines, except for SiHa, the most resistante cell line evaluated. In addition, although when compared to cisplatin, the crude extract showed a higher mean value of IC_{50} and had revealed an antagonistic effect in cisplatin drug combination, the crude extract promoted a large part of the important antineoplastic alterations evidenced for cisplatin such as cell motility and clonogenic potential inhibition, as well as signaling modulation. These results are in accordance with recent *in vitro* studies, which suggested that crude extracts of *A. crassiflora* may present tumor effects, such as glioma, melanoma, leukemia and lung, breast, ovarian cancer [9, 13, 14].

The phytochemical studies and FT-ICR MS analysis of the hexane partition revealed that it contains different classes of oxygenated compounds with carbon and oxygen numbers varying from C_{16} and O_2 to C_{42} and O_{10}, with DBE values between 1 and 23, with emphasis to fatty acids, acetogennins such as goniotrocin and coriaheptocin and alkaloids. The acetogenins present in the seed and fruits as well as the essential oil obtained from the leaves of *Annona* genus have also shown antitumor potential in various tumor types, incluiding anti-proliferative effect in cervical cancer [9, 45, 46]. Moreover, most of the observed efficacy of a crude extract could be result by a combined effect of more than one component. Therefore, the partition/fraction results may not always give a real efficacy of *in vivo* observation. Here, the hexane partition exhibited an IC_{50} average (5.53 μg/mL) significantly lower compared to the crude extract (16.32 μg/mL) and cisplatin (8.91 μg/mL), and was able to reduce approximately 90% the SiHa cells clonogenic potential suggesting a great tumorigenic activity from hexane partition and that great part of the metabolites present in the crude extract that are responsible for the antitumor potential might be present in the hexane partition.

We also interrogated the signaling pathways of cell proliferation and survival following the crude extract and the hexane partition exposure. Our results indicated that the crude extract induced lower levels of AKT protein activation and higher levels of ERK activation in both cell lines, suggesting to be a common mechanism of this extract. An increase in the activity of ERK was also verified after treatment with the hexane partition, at variance with the expression/activity of AKT that was not altered, indicating that the classes of secondary compounds found in this partition or the concentration used here are not able to promote AKT modulation as evidenced by crude extract. The ERK result is in accordance with the data in the literature about the mechanism of action of cisplatin, an agent that promotes DNA damage and culminates in activation of pro-apoptotic factors [47–50].

The expression of p21 protein, a cyclin-dependent kinase inhibitor, was also evaluated. Importantly, we showed for the first time that both crude extract and hexane partition

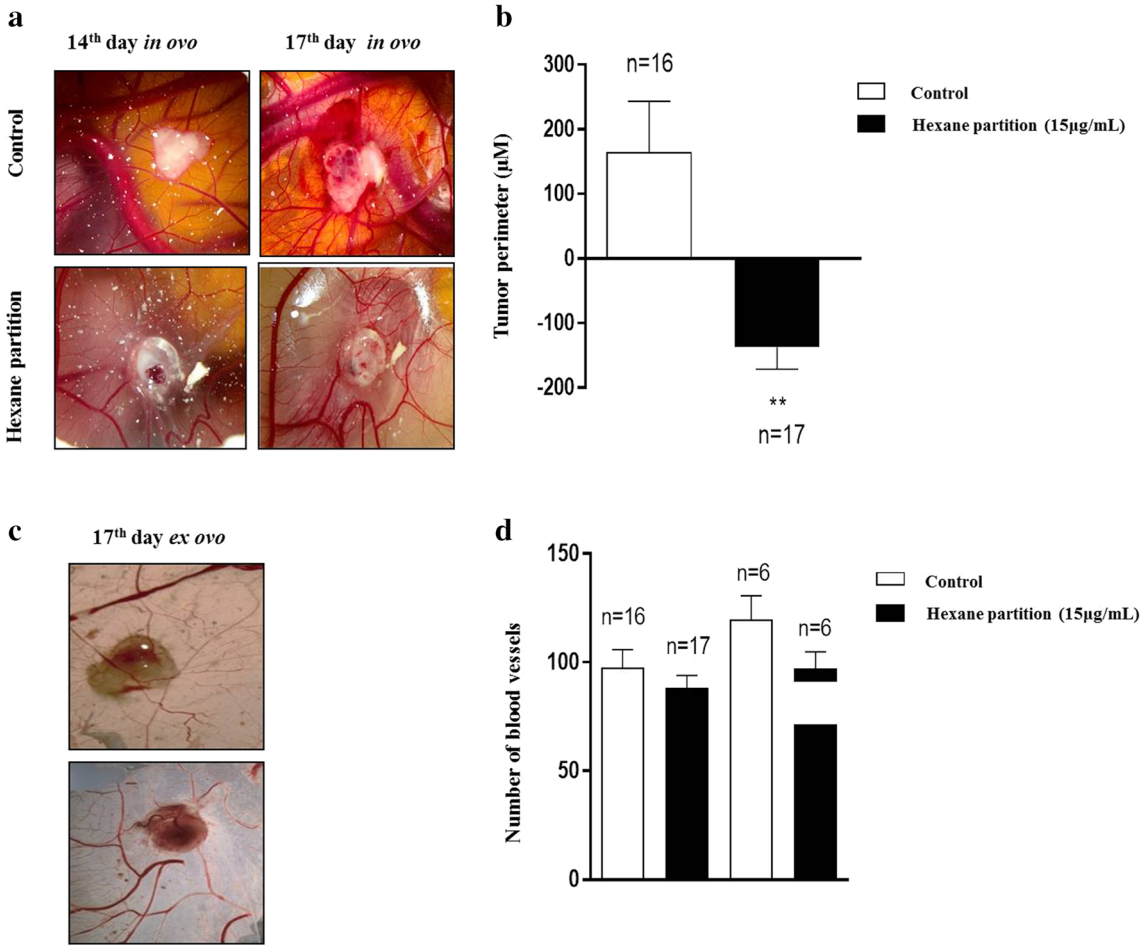

Fig. 6 In vivo effect of hexane partition treatment on tumor growth and angiogenesis of SiHa cell line. **a** Representative images of CAM assay at days 14 and 17 of tumor growth in ovo. **b** Tumor growth was measured by perimeter (μM) in ovo as described in methodology section. Data are representative of the mean percentage of tumor growth from day 14 (considered as 0%) to day 17 of development ± SD and the differences with $p < 0.05$ by Student's t-test were considered statistically significant. **c** In vivo effect of the hexane partition treatment in angiogenesis at day 17 of the SiHa cell line. Representative images of CAM assay at day 17 of ex ovo tumor growth. **d** The ex ovo blood vessel count was performed by ImageJ software. Data are representative of the mean number of vessels for each group of treatments = ± SD and the differences with $p < 0.05$ by Student's t-test were considered statistically significant

decreased p21 expression in SiHa cells by ubiquitin proteasome pathway (UPS). Interestingly, this effect was correlated to the downregulation of the activity of ERK and AKT. Otherwise, no different effect was observed in the activity of H2AX and PARP, indicating that the DNA damages or PARP activation are not inhibited by MG132 treatment. It is also known that p21 leads to arrest of the cell cycle in G1 phase, with inhibition of the replication process, and may induce cell death after treatment with antitumor drugs [51, 52]. The cell death findings indicate that treatment with the crude extract and the hexane partition induces apoptosis via the intrinsic pathway, through depolarization of the mitochondrial membrane and cleavage of caspases 3 and 9, as well as PARP.

Notably, several studies evidenciated the capacity of natural compounds to sensitize tumor cells from oxidative stress resulting in damage and cell death [53, 54]. In agreement with studies we investigated whether the damage suggested to the DNA, indicated by activation of the protein H2AX in both treatments, crude extract and the partition, was linked to the stress induced by ROS. Our results revealed that inhibition of ROS by NAC hindered the activation of the H2AX-induced by hexane partition, corroborating the literature that associates the increase in ROS to DNA damage [54]. However, the pretreatment with NAC was not able to alter the modulation of p21 and PARP, suggesting that hexane partition promotes cellular stress through ROS, which may act as causing damage, but not as direct modulator of the cell cycle and apoptosis, at least in the analyzed time and concentrations. Moreover, recent studies also support the existence of a new DNA repair pathway that involves degradation of p21. These mechanisms of regulation/verification allow cells to repair the DNA damage before the cell cycle progression is resumed, i.e., if the damage is too extensive, they may initiate apoptosis or cell senescence which supports our results [55].

Furthermore, through *in vivo* assay, we observed a significant decrease in the perimeter of SiHa tumors formed in the CAM, confirming the antitumoral activity of hexane partition on cervical cancer cells. Yet, the treatment did not affect angiogenesis, suggesting that the *in vivo* effect of the partition is directly related to tumor cytotoxicity, and not to a direct effect on chicken endothelial cells. Among the studies carried out for the family Annonaceae, leaf extract of *A. muricata* applied directly under the CAM exhibited a modulatory effect on angiogenesis in a dose-dependent manner, which was attributed to the presence of acetogenins [56]. Similarly, several other phytochemical compounds, such as polyphenols, flavonoids and chalcones, have been shown to influence angiogenesis [57, 58]. Although our phytochemical studies of the hexane partition of *A. crassiflora* have revealed the presence of several classes of these compounds, such as flavonoids and acetogenins, no evidence was found for an effect on angiogenesis during development of the cervical cancer tumor. Regarding *A. crassiflora* extract, Pimenta and collaborators demonstrated the reduction of Ehrlich solid tumors upon treatment with a partition rich in acetogenins [14].

In conclusion, our study represents a comphreensive characterization of antitumor mechanisms associated to the extract and its partition of *A. crassiflora* Mart. in cervical cancer. The results revealed that the crude extract, and mainly its hexanic partition significantly alters cell viability, proliferation and migration, and induces cell death via intrinsic pathway in cervical cancer cell lines. Moreover, the hexane partition display antitumoral effect *in vivo* in cervical cancer cells. These results provide evidences for further *in vitro* and *in vivo* analysis of hexane partition of *A. crassiflora* Mart. as an antineoplastic agent for cervical cancer.

Author contributions Viviane A O Silva designed all the experiments as well as participated of data acquisition, its interpretation and drafted the manuscript. Viviane A O Silva, Ana Laura V Alves and Marcela N Rosa carried out the studies of cell culture including cytotoxicity and proliferation assay, wound healing migration assay, colony formation assay, and statistical analysis from Hexane partition. Viviane A O Silva, Marcela N Rosa and Larissa R V Silva carried out the studies of cell culture including cytotoxicity and proliferation assay, wound healing migration assay, drug combination studies and statistical analysis from crude extract. Aline Tansini helped to carry out flow cytometry assays and its interpretation. Matias Melendez, Giovanna Longato and Olga Martinho contributed to design some experiments, interpretation of data and involved in revising critically the manuscript. Ana Laura V Alves and Fernanda Cury helped to design and performed the *in vivo* experiments. Bruno G. Oliveira, Fernanda E. Pinto and Wanderson Romãohas been responsible for the preparation of extracts. Izabela Faria Gomes contributed to design some experiments and analysed about the profile of secondary compounds identified in the hexane partition. Rosy Ribeiro conceived the extracts and partition, participated in its design, interpretation of data. Rui Manuel Reis conceived the study, participated in its design and coordination, interpretation of data, drafted the manuscript and have been involved in revising it critically for important intellectual content. All authors read and approved the final manuscript.

Funding This study was supported by grants from the FINEP (MCTI/FINEP/MS/SCTIE/DECIT-01/2013 - FPXII-BIOPLAT), CAPES, FAPEMIG, UFSJ and Barretos Cancer Hospital, all from Brazil.

Compliance with ethical standards

Conflict of interest The authors confirm that this article content has no conflicts of interest.

Ethical approval All applicable international, national, and/or institutional guidelines for the care and use of animals were followed. All procedures performed in studies involving animals were in accordance with the ethical standards of the institution or practice at which the studies were conducted. This article does not contain any studies with human participants performed by any of the authors.

Informed consent Informed consent was obtained from all individual participants included in the study.

References

1. Siegel RL, Miller KD, Jemal A (2017) Cancer statistics, 2017. CA Cancer J Clin 67(1):7–30. https://doi.org/10.3322/caac.21387
2. Catarino R, Petignat P, Dongui G, Vassilakos P (2015) Cervical cancer screening in developing countries at a crossroad: emerging technologies and policy choices. World J Clin Oncol 6(6):281–290. https://doi.org/10.5306/wjco.v6.i6.281
3. Florea AM, Busselberg D (2011) Cisplatin as an anti-tumor drug: cellular mechanisms of activity, drug resistance and induced side effects. Cancers 3(1):1351–1371. https://doi.org/10.3390/cancers3011351
4. Newman DJ, Cragg GM (2016) Natural products as sources of new drugs from 1981 to 2014. J Nat Prod 79(3):629–661. https://doi.org/10.1021/acs.jnatprod.5b01055
5. Butler MS, Robertson AA, Cooper MA (2014) Natural product and natural product derived drugs in clinical trials. Nat Prod Rep 31(11):1612–1661. https://doi.org/10.1039/c4np00064a
6. Dutra RC, Campos MM, Santos AR, Calixto JB (2016) Medicinal plants in Brazil: pharmacological studies, drug discovery, challenges and perspectives. Pharmacol Res 112:4–29. https://doi.org/10.1016/j.phrs.2016.01.021
7. de Melo JG, Santos AG, de Amorim EL, do Nascimento SC, de Albuquerque UP (2011) Medicinal plants used as antitumor agents in Brazil: an ethnobotanical approach. Evid Based Complement Alternat Med 2011:365359. https://doi.org/10.1155/2011/365359
8. Lopes JC, Mello-Silva R (2014) Diversity and characterization of Annonaceae from Brazil. Rev Bras Frutic 36:125–131. https://doi.org/10.1590/S0100-29452014000500015
9. Tundis R, Xiao J, Loizzo MR (2017) Annona species (Annonaceae): a rich source of potential antitumor agents? Ann N Y Acad Sci 1398(1):30–36. https://doi.org/10.1111/nyas.13339
10. Chatrou LWP, D M, Erkens RHJ, Couvreur TLP, Neubig KM, Abbott JR, Mols JB, Maas JW, Saunders RMK, Chase MW (2012) A new subfamilial and tribal classification of the pantropical flowering plant family Annonaceae informed by molecular phylogenetics. Bot J Linn Soc 169:5–40
11. Pimenta LP, Garcia GM, Goncalves SG, Dionisio BL, Braga EM, Mosqueira VC (2014) In vivo antimalarial efficacy of acetogenins, alkaloids and flavonoids enriched fractions from Annona crassiflora

Mart. Nat Prod Res 28(16):1254–1259. https://doi.org/10.1080/14786419.2014.900496
12. Rocha RS, Kassuya CAL, Formagio ASN, Mauro MO, Andrade-Silva M, Monreal ACD, Cunha-Laura AL, Vieira MC, Oliveira RJ (2016) Analysis of the anti-inflammatory and chemopreventive potential and description of the antimutagenic mode of action of the Annona crassiflora methanolic extract. Pharm Biol 54(1):35–47
13. Formagio AS, Vieira MC, Volobuff CR, Silva MS, Matos AI, Cardoso CA, Foglio MA, Carvalho JE (2015) In vitro biological screening of the anticholinesterase and antiproliferative activities of medicinal plants belonging to Annonaceae. Braz J Med Biol Res 48(4):308–315. https://doi.org/10.1590/1414-431X20144127
14. Pimenta L, Mendonça D, Pretti D, Cruz B, Leite E, De Oliveira M (2011) Evaluation of in vivo antitumor activity of *Annona crassiflora* wood extract. IJPSDR 3(3):270–273
15. Silva-Oliveira RJ, Silva VA, Martinho O, Cruvinel-Carloni A, Melendez ME, Rosa MN, de Paula FE, de Souza Viana L, Carvalho AL, Reis RM (2016) Cytotoxicity of allitinib, an irreversible anti-EGFR agent, in a large panel of human cancer-derived cell lines: KRAS mutation status as a predictive biomarker. Cell Oncol (Dordr) 39(3):253–263. https://doi.org/10.1007/s13402-016-0270-z
16. Silva VAO, Rosa MN, Miranda-Goncalves V, Costa AM, Tansini A, Evangelista AF, Martinho O, Carloni AC, Jones C, Lima JP, Pianowski LF, Reis RM (2018) Euphol, a tetracyclic triterpene, from Euphorbia tirucalli induces autophagy and sensitizes temozolomide cytotoxicity on glioblastoma cells. Investig New Drugs. https://doi.org/10.1007/s10637-018-0620-y
17. Moniz S, Martinho O, Pinto F, Sousa B, Loureiro C, Oliveira MJ, Moita LF, Honavar M, Pinheiro C, Pires M, Lopes JM, Jones C, Costello JF, Paredes J, Reis RM, Jordan P (2013) Loss of WNK2 expression by promoter gene methylation occurs in adult gliomas and triggers Rac1-mediated tumour cell invasiveness. Hum Mol Genet 22(1):84–95. https://doi.org/10.1093/hmg/dds405
18. Martinho O, Silva-Oliveira R, Miranda-Goncalves V, Clara C, Almeida JR, Carvalho AL, Barata JT, Reis RM (2013) In vitro and in vivo analysis of RTK inhibitor efficacy and identification of its novel targets in Glioblastomas. Transl Oncol 6(2):187–196
19. Chou TC, Talalay P (1984) Quantitative analysis of dose-effect relationships: the combined effects of multiple drugs or enzyme inhibitors. Adv Enzym Regul 22:27–55
20. Liu J, Cooks RG, Ouyang Z (2011) Biological tissue diagnostics using needle biopsy and spray ionization mass spectrometry. Anal Chem 83(24):9221–9225. https://doi.org/10.1021/ac202626f
21. Pinheiro MLB, Xavier CM, ADLd S, Rabelo DM, Batista CL, Batista RL, Costa EV, Campos FR, Barison A, Valdez RH, Ueda-Nakamura T, Nakamura CV (2009) Acanthoic acid and other constituents from the stem of Annona amazonica (Annonaceae). J Braz Chem Soc 20:1095–1102
22. Alali FQ, Liu XX, McLaughlin JL (1999) Annonaceous acetogenins: recent progress. J Nat Prod 62(3):504–540. https://doi.org/10.1021/np980406d
23. FMAd S, Koolen HHF, RAd A, ADLd S, Pinheiro MLB, Costa EV (2012) Desreplicação de alcaloides aporfínicos e oxoaporfínicos de Unonopsis guatterioides por ESI-IT-MS. Quim Nova 35:944–947
24. Etcheverry S, Saphaz S, Fall D, Laurens A, Cavé A (1995) Annoglaucin, an acetogenin from *Annona glauca*. Phytochemistry 35(6):1423–1426. https://doi.org/10.1016/0031-9422(94)00820-j
25. FdCd N, Boaventura MAD, Assunção ACS, Pimenta LPS (2003) Acetogeninas de anonáceas isoladas de folhas de Rollinia laurifolia. Quím Nova 26:319–322
26. Lin RJ, Wu MH, Ma YH, Chung LY, Chen CY, Yen CM (2014) Anthelmintic activities of aporphine from Nelumbo nucifera Gaertn. cv. Rosa-plena against Hymenolepis nana. Int J Mol Sci 15(3):3624–3639. https://doi.org/10.3390/ijms15033624
27. TJ CVCO, Queiroga CS, MVS C-B, MFFM D, CUGBd L, BVdO S, JCLR P, MSd S, IMF S (2012) Chemical constituents of the leaves from *Rollinia leptopetala* R. E. Fries. Quím Nova 35:138–142. https://doi.org/10.1590/S0100-40422012000100025
28. Silva FMA, Silva Filho FA, Lima BR, Almeida RA, Soares ER, Koolen HHF, Souza ADL, Pinheiro MLB (2016) Chemotaxonomy of the Amazonian *Unonopsis* species based on leaf alkaloid fingerprint direct infusion ESI-MS and chemometric analysis. J Braz Chem Soc 27:599–604
29. Alali FQ, Kaakeh W, Bennett GW, McLaughlin JL (1998) Annonaceous acetogenins as natural pesticides: potent toxicity against insecticide-susceptible and -resistant German cockroaches (Dictyoptera: Blattellidae). J Econ Entomol 91(3):641–649
30. Mo S, Dong L, Hurst WJ, van Breemen RB (2013) Quantitative analysis of phytosterols in edible oils using APCI liquid chromatography-tandem mass spectrometry. Lipids 48(9):949–956. https://doi.org/10.1007/s11745-013-3813-3
31. FMAd S, BRd L, Soares ER, RAd A, FAd SF, Corrêa WR, Salvador MJ, AQLd S, Koolen HHF, ADLd S, Pinheiro MLB (2015) Polycarpol in Unonopsis, Bocageopsis and Onychopetalum Amazonian species: chemosystematical implications and antimicrobial evaluation. Rev Bras 25:11–15
32. Wele A, Zhang Y, Caux C, Brouard J-P, Dubost L, Guette C, Pousset J-L, Badiane M, Bodo B (2002) Isolation and structure of cyclosenegalins a and B, novel cyclopeptides from the seeds of Annona senegalensis. J Chem Soc Perkin Trans 1(23):2712–2718. https://doi.org/10.1039/B205035H
33. Hisham A, Sunitha C, Sreekala U, Pieters L, De Bruyne T, Van den Heuvel H, Claeys M (1994) Reticulacinone, an acetogenin from Annona reticulata. Phytochemistry 35(5):1325–1329. https://doi.org/10.1016/S0031-9422(00)94847-7
34. Wiart C, Martin MT, Awang K, Hue N, Serani L, Laprevote O, Pais M, Rhamani M (2001) Sesquiterpenes and alkaloids from Scorodocarpus borneensis. Phytochemistry 58(4):653–656
35. Karapandzova M, Stefkov G, Cvetkovikj I, Stanoeva JP, Stefova M, Kulevanova S (2015) Flavonoids and other phenolic compounds in needles of Pinus peuce and other pine species from the Macedonian Flora. Nat Prod Commun 10(6):987–990
36. Da Silva ELM, Roblot F, Laprévote O, Sérani L, Cavé A (1997) Coriaheptocins A and B, the first Heptahydroxylated Acetogenins, isolated from the roots of Annona coriacea. J Nat Prod 60(2):162–167. https://doi.org/10.1021/np9606660
37. Rockenbach II, Jungfer E, Ritter C, Santiago-Schübel B, Thiele B, Fett R, Galensa R (2012) Characterization of flavan-3-ols in seeds of grape pomace by CE, HPLC-DAD-MSn and LC-ESI-FTICR-MS. Food Res Int 48(2):848–855. https://doi.org/10.1016/j.foodres.2012.07.001
38. Etse JT, Gray AI, Lavaud C, Massiot G, Nuzillard J-M, Waterman PG (1991) Chemistry of the annonaceae, part 29. Structure of mezzettiaside-2, −4, −5, −6 and −7, new partially esterified 1-O-octyl tri- and tetra-rhamnosyl derivatives from Mezzettia leptopoda. J Chem Soc Perkin Trans 1(4):861–864. https://doi.org/10.1039/P19910000861
39. Gartel AL, Tyner AL (2002) The role of the cyclin-dependent kinase inhibitor p21 in apoptosis. Mol Cancer Ther 1(8):639–649
40. Bendjennat M, Boulaire J, Jascur T, Brickner H, Barbier V, Sarasin A, Fotedar A, Fotedar R (2003) UV irradiation triggers ubiquitin-dependent degradation of p21(WAF1) to promote DNA repair. Cell 114(5):599–610
41. Fragkos M, Jurvansuu J, Beard P (2009) H2AX is required for cell cycle arrest via the p53/p21 pathway. Mol Cell Biol 29(10):2828–2840
42. Martin-Cordero C, Leon-Gonzalez AJ, Calderon-Montano JM, Burgos-Moron E, Lopez-Lazaro M (2012) Pro-oxidant natural products as anticancer agents. Curr Drug Targets 13(8):1006–1028
43. Kuete V, Seo EJ, Krusche B, Oswald M, Wiench B, Schroder S, Greten HJ, Lee IS, Efferth T (2013) Cytotoxicity and pharmacogenomics of medicinal plants from traditional korean

medicine. Evid Based Complement Alternat Med 2013:341724. https://doi.org/10.1155/2013/341724
44. JM SMAP (1990) Assays related to cancer drug discovery. In: HOSTETTMANN K (ed) Methods in plant biochemistry: assays for bioactivity. Academic Press, London, pp 71–133
45. Matsushige A, Kotake Y, Matsunami K, Otsuka H, Ohta S, Takeda Y (2012) Annonamine, a new aporphine alkaloid from the leaves of Annona muricata. Chem Pharm Bull 60(2):257–259
46. Xu L, Li K, Sun N, Kong J (1992) Alkaloids of Annona reticulata L. Zhongguo Zhong Yao Za Zhi 17(5):295–296 inside backcover
47. Wang X, Martindale JL, Holbrook NJ (2000) Requirement for ERK activation in cisplatin-induced apoptosis. J Biol Chem 275(50): 39435–39443. https://doi.org/10.1074/jbc.M004583200
48. Brozovic A, Osmak M (2007) Activation of mitogen-activated protein kinases by cisplatin and their role in cisplatin-resistance. Cancer Lett 251(1):1–16. https://doi.org/10.1016/j.canlet.2006.10.007
49. Abbas T, Dutta A (2009) p21 in cancer: intricate networks and multiple activities. Nat Rev Cancer 9(6):400–414. https://doi.org/10.1038/nrc2657
50. Cagnol S, Chambard JC (2010) ERK and cell death: mechanisms of ERK-induced cell death–apoptosis, autophagy and senescence. FEBS J 277(1):2–21. https://doi.org/10.1111/j.1742-4658.2009.07366.x
51. Gartel AL, Radhakrishnan SK (2005) Lost in transcription: p21 repression, mechanisms, and consequences. Cancer Res 65(10): 3980–3985. https://doi.org/10.1158/0008-5472.CAN-04-3995
52. Liu G, Lozano G (2005) p21 stability: linking chaperones to a cell cycle checkpoint. Cancer Cell 7(2):113–114
53. Atoui AK, Mansouri A, Boskou G, Kefalas P (2005) Tea and herbal infusions: their antioxidant activity and phenolic profile. Food Chem 89(1):27–36
54. Sznarkowska A, Kostecka A, Meller K, Bielawski KP (2017) Inhibition of cancer antioxidant defense by natural compounds. Oncotarget 8(9):15996–16016. https://doi.org/10.18632/oncotarget.13723
55. Liu S, Bishop WR, Liu M (2003) Differential effects of cell cycle regulatory protein p21(WAF1/Cip1) on apoptosis and sensitivity to cancer chemotherapy. Drug Resist Updat 6(4):183–195. https://doi.org/10.1016/S1368-7646(03)00044-X
56. Martinho O, Pinto F, Granja S, Miranda-Goncalves V, Moreira MA, Ribeiro LF, di Loreto C, Rosner MR, Longatto-Filho A, Reis RM (2013) RKIP inhibition in cervical cancer is associated with higher tumor aggressive behavior and resistance to cisplatin therapy. PLoS One 8(3):e59104. https://doi.org/10.1371/journal.pone.0059104
57. Mojzis J, Varinska L, Mojzisova G, Kostova I, Mirossay L (2008) Antiangiogenic effects of flavonoids and chalcones. Pharmacol Res 57(4):259–265. https://doi.org/10.1016/j.phrs.2008.02.005
58. Staton CA, Reed MW, Brown NJ (2009) A critical analysis of current in vitro and in vivo angiogenesis assays. Int J Exp Pathol 90(3):195–221. https://doi.org/10.1111/j.1365-2613.2008.00633.x